A Study on the Deployment and Cooperative Operation of Ultra-Dense Networks

YANPENG YANG

Licentiate Thesis in Information and Communication Technology
School of Information and Communication Technology
KTH Royal Institute of Technology
Stockholm, Sweden 2017

KTH School of Information and
Communication Technology
SE-164 40 Kista
SWEDEN

TRITA-ICT 2017:03
ISBN 978-91-7729-260-9

Akademisk avhandling som med tillstånd av Kungl Tekniska högskolan framlägges till offentlig granskning för avläggande av licentiatexamen i Informations- och kommunikationsteknik fredagen den 17 february 2017 klockan 13:00 i Sal B, Electrum, Kungl Tekniska högskolan, Kistagången 16, Kista.

© Yanpeng Yang, February 2017

Tryck: Universitetsservice US AB

Abstract

The traffic volume in wireless communication has grown dramatically in the last decade. Recent predictions indicate such data storm will be even more violent in the short run. Potential solutions for accommodating the rapid traffic growth can be summed up into three categories: broadening the available bandwidth, improving the spectral efficiency, and densifying the infrastructure. In this thesis, we focus on the densification dimension which has been proved to be the most effective in the past. The current gain of network densification mainly comes from cell splitting, thereby serving more user equipments (UEs) simultaneously. This trend will decelerate as base station (BS) density gets closer to or even surpass UE density which forms a ultra-dense network (UDN). Thus, it is crucial to understand the behavior of ultra-densification for future network provisioning.

An important question for future system design and operating strategy is which element is more effective than others. To this end, we start from comparing the effectiveness of densification with spectrum expansion and multi-antenna systems in terms of meeting certain traffic demand. Our findings show that deploying more BSs provides a substantial gain in sparse network but the gain decreases progressively in a UDN. Therefore, adding multi-antennas on BSs or utilizing additional spectrum are more favorable than further densification in a UDN. The impact of traffic types is also discussed. Even with the same area throughput, different combinations of individual throughput and UE density lead to different requirements for resources.

The diminishing gain appears in a UDN make us curious to know if there exists a terminal on the way of densification. Such uncertainty leads to the study on the asymptotic behavior of densification in the next part of the thesis. We incorporate a sophisticated bounded dual-slope path loss model and practical UE densities in our analysis. By using stochastic geometry, we derive the expressions of the coverage probability of a typical UE and network area spectral efficiency (ASE). In addition, we present the asymptotic behavior of ultra-densification: the coverage probability and ASE have non-zero convergence in asymptotic regions unless UE density goes to infinity (full load).

Previous UDN studies focus on single BS association rule which results in a large portion of dormant BSs in the network. Thus, whether we can utilize these dormant BSs to improve system performance is an interesting question. To this end, we employ joint transmission (JT) techniques into a UDN. Two types of cooperation schemes are investigated: non-coherent JT and coherent JT depending on the availability of channel state information (CSI). Our results reveal that non-coherent JT is not beneficial in a UDN due to the simultaneous increase in both desired signal and interference. Coherent cooperative transmissions with CSI are able to increase UE spectral efficiency (SE) depending on the environmental characteristics captured by critical distance and path loss exponents.

Sammanfattning

Trafikvolymen inom trådlös kommunikation har ökat dramatiskt det senaste årtiondet och de senaste prognoserna visar på en fortsatt kraftig ökning på kort sikt. Potentiella lösningar för att kunna tillgodose den snabba trafikökningen kan sammanfattas i tre kategorier: utöka den tillgängliga bandbredden, förbättra spektraleffektiviteten, och förtäta infrastrukturen. I denna avhandling fokuserar vi på förtätning som historiskt har visat sig vara den mest givande lösningen. Prestandavinsten av nätverksförtätning kommer huvudsakligen från celldelning som tillåter fler användarterminaler (UE) att tjänas samtidigt. Den här trenden bromsas dock upp när basstationstätheten går mot eller till och med överstiger UE-tätheten och formar ett ultratätt nätverk (UDN). Det är därmed viktigt att förstå beteendet av ultraförtätning för framtida nätverkstillhandahållning.

En viktig fråga för framtida systemdesign och operativ strategi ligger i att bestämma vilken komponent som är den mest effektiva. För detta ändamål jämför vi verkningsfullheten av förtätning med spektrumutökning och multiantennsystem i syfte att tillgodose vissa trafikkrav. Våra resultat visar att förlägga fler basstationer (BS) ger en påtaglig förbättring i glesare nätverk som dock minskar progressivt i UDN. Att inkludera fler basstationsantenner eller tillgodoräkna sig mer bandbredd blir då mer fördelaktigt än fortsatt förtätning i UDN. Inverkan av trafiktyp diskuteras också. Även med samma dataflöde per areaenhet så leder olika kombinationer av individuella dataflöden och användartäthet till olika resurskrav.

Den minskande prestandavinsten i UDN leder till frågan huruvida det finns en ändpunkt på vägen till förtätning. Denna osäkerhet leder oss till att studera asymptotiskt beteende av förtätning i nästa del av avhandlingen. Vi införlivar en sofistikerad tvådelad sträckdämpningsmodell och praktiska UE-tätheter i vår analys. Med hjälp av stokastisk geometri härleder vi uttryck för täckningssannolikhet för en typisk UE och areaspektraleffektiviteten (ASE) för nätverket. Därutöver presenterar vi asymptotiskt beteende av ultraförtätning: täckningssannolikhet och ASE har en konvergens skild från noll i det asymptotiska fallet såvida inte UE-tätheten går mot oändligheten (full last).

Tidigare studier av UDN har fokuserat på association med en enda BS vilket resulterar i en stor andel vilande BSs i ett nätverk. Huruvida man kan nyttiggöra dessa vilande BSs för att förbättra prestanda är en intressant frågeställning. För detta ändamål begagnar vi oss av gemensam transmission (JT) i UDN. Två typer av kooperativa uppställningar undersöks: JT och koherent JT beroende på tillgänglighet av kanalkännedom (CSI). Våra resultat visar att icke-koherent JT inte är fördelaktigt i UDN till följd av ökning i både önskad signal men också störningar. Koherent kooperativ transmission med CSI kan förbättra en UE:s spektraltäthet (SE) beroende på omgivningens karaktär i form av kritiskt avstånd och sträckdämpningsexponent.

Acknowledgements

By writing this thesis, I have passed half way of my PhD journey. I would like to acknowledge people who have helped me on my way to the destination. First, I express my sincere gratitude to Dr. Ki Won Sung and Prof. Jens Zander for let me start this wonderful journey in RSlab as well as METIS project for the research funding. I owe my biggest thanks to my main advisor Dr. Ki Won Sung, for your patient guidance, encouragement and valuable feedbacks on my work. I am deeply grateful to my co-advisor Prof. Jens Zander for broadening my view of research and inspiring me the way of thinking. I greatly appreciate Dr. Du Ho Kang and Prof. Ben Slimane for reviewing my Licentiate proposal and Licentiate thesis and providing valuable comments. I would like to offer my special thanks to Dr. Yngve Selén for accepting to be my opponent on my Licentiate defense.

I would like to thank all my colleagues in RSlab for providing a great research environment and nice discussions with me. My special thanks to Prof. Seong-Lyun Kim from Yonsei University for accepting me as a visit PhD student in his lab and Dr. Jihong Park for all his beneficial comments on my work. I also feel grateful to the former members of RSlab for setting good examples to me on the research journey. Another credits should be given to the PhD office and ITservice center for their excellent administrative support.

Last but by no means least, it is impossible to describe my gratefulness to my parents and my girlfriend Jie, for their support, encouragement, patience and endless love.

Yanpeng Yang,
Stockholm, Feb. 2017

Contents

Contents **ix**

List of Figures **xi**

List of Tables **xii**

I Thesis Overview **1**

1 Introduction **3**
1.1 Background . . . 3
1.2 Related Works . . . 5
1.2.1 From dense to ultra-dense network . . . 5
1.2.2 Modeling ultra-dense networks . . . 6
1.3 Thesis Focus and Problem Formulation . . . 7
1.4 Overview of Thesis Contributions . . . 9
1.5 Thesis Outline . . . 10

2 Modeling and Methodology **13**
2.1 Introduction . . . 13
2.2 Network modeling with stochastic geometry . . . 14
2.3 Pros and cons of stochastic geometry approach . . . 16

3 Resource Trade-offs in Network Provisioning **17**
3.1 System model . . . 17
3.2 Technical Rate of Substitution . . . 18
3.3 Key results . . . 19
3.3.1 TRS of densification . . . 19
3.3.2 Impact of traffic types . . . 20
3.4 Summary . . . 21

4 Asymptotic Behavior of Densification **23**
4.1 Bounded dual-slope path loss model . . . 23

4.2 Key results 25
4.3 Summary 26

5 Cooperative transmissions in UDN **29**
5.1 System model 29
5.2 Cooperative transmission models 30
5.2.1 Cooperation schemes 30
5.2.2 Cooperation Gains 31
5.3 Key results 31
5.4 Summary 33

6 Conclusion and Future Work **35**
6.1 Concluding remarks 35
6.2 Future works 36

Bibliography **37**

List of Figures

1.1 Resource requirement in different traffic demands. 4
1.2 Evolution from sparse network to ultra-dense network 5
1.3 Approaches in propagation and load modeling 6

2.1 Network topology based on the PPP assumption 14

3.1 Relation between antenna number and BS density. (©2015 IEEE.) . . . 19
3.2 Relation between spectrum and BS density. (©2015 IEEE.) 20
3.3 Resource requirement in different traffic demands. (©2015 IEEE.) . . . 21

4.1 A bounded dual-slope path loss model 24
4.2 Effect of λ_u on coverage probability under bounded dual-slope model. . 25
4.3 ASE bounds and comparison with previous models. 27

5.1 UE-centric Voronoi cells for modeling cooperative transmissions in a UDN. 30
5.2 User performance with different critical distances when path loss exponents=[2,4], $\lambda_b = 4000/\text{km}^2$, $\lambda_u = 200/\text{km}^2$. 32
5.3 Cooperation gain with different dual-slope exponents $[\alpha_1, \alpha_2]$ when $\lambda_b = 4000/\text{km}^2$, $\lambda_u = 200/\text{km}^2$, $R_c = 70\text{m}$. 32
5.4 Cooperation gain with different UE densities when path loss exponents = [2,4], $\lambda_b = 4000/\text{km}^2$, $R_c = 70\text{m}$, $N = 5$. 33
5.5 Cooperation gain with different BS densities when path loss exponents = [2,4], $\lambda_u = 200/\text{km}^2$, $R_c = 70\text{m}$, $N = 5$. 34

List of Tables

3.1 TRS between antenna number and densification ($\frac{\triangle M}{\triangle \lambda_b}$). (©2015 IEEE.) 19
3.2 TRS between spectrum and densification ($\frac{\triangle \text{MHz}}{\triangle \lambda_b}$). (©2015 IEEE.) . . . 20

Part I

Thesis Overview

Chapter 1

Introduction

1.1 Background

The wireless communication demand has experienced explosive growth during the last decades and is expected to keep increasing in the near future. High quality services such as high definition (HD) videos and real-time broadcasting are required on the wireless devices, which are supported by high data rates [1]. Also, the number of connected machine-type devices serving Internet of Things (IoT), is expected to be nearly 7 billion in 2020 [2]. To accommodate such rapid traffic growth, the fifth generation (5G) of wireless networks are expected to improve the network capacity by 1000 times compared with that in 2010 [3] [4], which poses a tremendous challenge to wireless research community. An industry consensus is that three fundamental ingredients are available for increasing wireless network capacity thereby achieving the 1000 capacity gains, which are categorized as follows and shown in Fig. 1.1 [5]:

- Spectrum Expansion, to seek more spectrum such as exploring millimeter wave spectrum and/or the unlicensed bands;
- Spectral Efficiency Enhancement, to design advanced physical layer techniques to support high transmission rate, such as efficient modulation and coding schemes, cooperative transmissions and massive Multiple-Input Multiple-Output (MIMO);
- Spatial Spectrum Reuse, to improve the spectrum reuse per unit area by densely deploying base stations (BSs), i.e., network densification.

Spectrum is considered as a virtual resource, which is different from the other two elements implemented in the infrastructures. In Shannon's formula, the additional bandwidth can lead to an almost linear increase in data capacity (especially in interference limited system). However, acquisition of more bandwidth is a very costly solution, unless devices are authorized for spectrum sharing or operating in

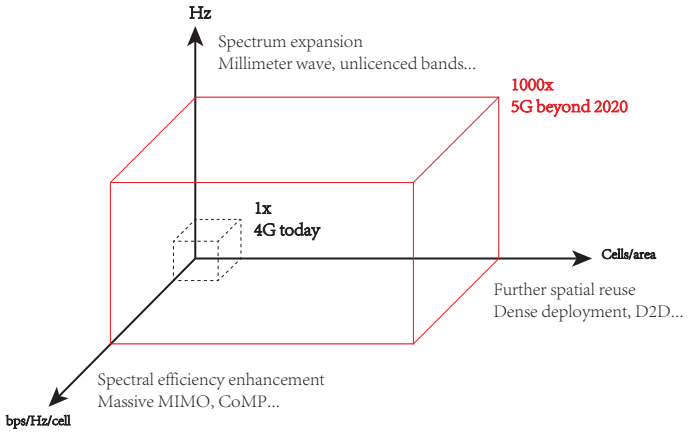

Figure 1.1: Resource requirement in different traffic demands.

unlicensed bands. Meanwhile, recent studies show that point-to-point link throughput is close to the theoretical limits [6]. With this regard, multi-antenna or even massive MIMO system is considered to provide extra capacity. By adding multiple antennas, it offers a spatial dimension in addition to time and frequency for communication and yields a degree of freedom gain to accommodate more information data. With massive MIMO, a performance improvement can be obtained with regard to reliability, spectral efficiency, and energy efficiency [7] [8]. Nevertheless, the performance of massive MIMO may be limited by the finite and potentially correlated scattering given the space constraints and pilot contamination issues [8].

Densely deployed small cells are motivated by increasing the reuse of spectrum in the network area. It can decrease the number of user equipment (UE) at each BS, thereby reducing the competition for resources. There are several advantages of network densification. First, the cost of small cell deployment is much lower than the other two options. Both capital expenditure (CAPEX) and operational expenditure (OPEX) of deploying small cells are considerably low compared to multi-antenna macro-BS deployment [9], where a significant portion of the recurring cost comes from wired backhauling, power usage, and real estate [10]. Furthermore, small cells are energy efficient as they can be utilized intelligently and opportunistically. Depending on the traffic demand, small cells can turn into sleep mode so that the energy consumption and interference can be reduced. At last, by deploying small cells over the macro-cell umbrella heterogeneously, cell edge may become vague or even vanished. The 'poor cell edge UEs' will experience good throughput over the network.

According to Martin Cooper, the pioneer and visionary, the wireless capacity has doubled about every two years and increased around 1,000,000 fold from 1950

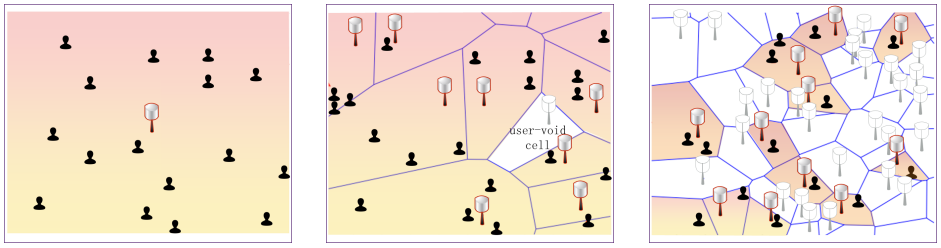

(a) Sparse network (b) Small cells (c) UDN

Figure 1.2: Evolution from sparse network to ultra-dense network

to 2000, also known as 'Cooper's Law'. The 1 million gains are composed by 25x improvement from wider spectrum, 25x improvement from advanced modulation and coding schemes, and an astonishing 1600x improvement brought by deploying more BSs and reducing cell size [11]. By this taken, network densification has made significant contributions to capacity improvement in the past and is anticipated to play an important role in the future.

1.2 Related Works

1.2.1 From dense to ultra-dense network

Network densification has been employed over several cellular generations [12]. The first generation (1G) mobile networks in the 1980s, had cell radius on the order of tens of kms. Since then, the cell sizes have been progressively shrinking. Nowadays, networks are rapidly evolving to include nested small cells such as pico-cells (range below 200 meters) and femto-cells (range under 20 meters), as well as distributed antenna systems [13] [14] [15]. Such small cells are equipped with agile antennas in replacing traditional bulky transceiver units and can be installed arbitrarily for various scenarios [16]. To this end, there is a growing amount of research on small cells. For instance, the interference mitigation methods are investigated in [17, 18]; the energy efficiency problems are specifically studied in [19–21]; the backhauling for small cells are discussed in [22, 23]

The studies above are based on the assumptions of fully loaded network where all the BSs have at least one UE to serve. However, as densification goes further, some cells may have no UE inside and become idle which is illustrated in Fig. 1.2. When the BS density is sufficiently large, there will be a body of void cells in the network. Such scenario is termed as ultra-dense network (UDN) [24], of which the definition is given as:

A cellular network with BS density λ_b and active UE density λ_u is called a UDN where $\rho \triangleq \frac{\lambda_b}{\lambda_u} \gg 1$. The notation $f \gg g$ implies f is sufficiently large so that $O(g/f)$ is approximated by 0.

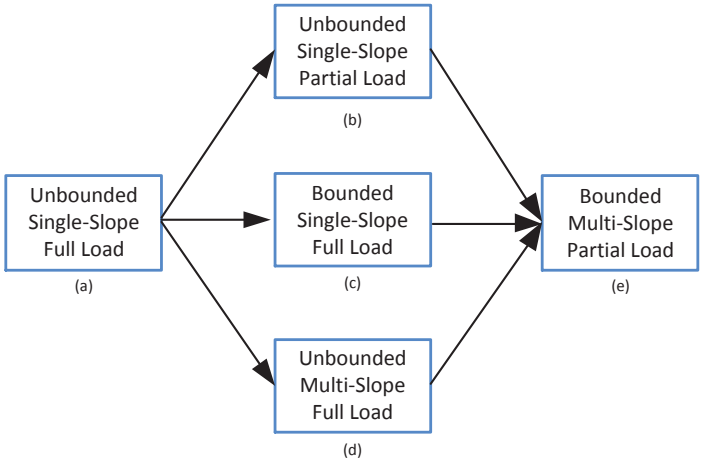

Figure 1.3: Approaches in propagation and load modeling

Based on the given definition, lots of existing theorems and conclusions applied to current macro cellular networks or even small cells may not hold in UDN scenarios because not all the BSs are transmitting. Thus, the advantage of densification may become questionable in a UDN.

1.2.2 Modeling ultra-dense networks

In order to understand the impact of network densification, quantitative as well as scalable research is indispensable. A glance at the approaches in previous works is illustrated in Fig. 1.3, in which the assumptions of propagation environment and network load condition are the key distinctions. Starting from step (a), [25] provides a comprehensive understanding on the impact of BS density in fully loaded downlink cellular networks with a simple single-slope path loss model. It concludes that BS densification does not change the coverage probability of individual UE (in interference-limited networks), but linearly improves the area spectral efficiency (ASE) defined as the sum average spectral efficiency of all active BSs achieving the target threshold in a unit area sum rate. However, this conclusion may become invalid in a UDN due to its too simplified signal propagation and load models.

To examine the impact of ultra densification, it is important to incorporate the propagation characteristics of UDN properly. It is well known that the path loss exponent is small (or large) when radio signals experience less (or more) absorption and diffraction losses. In a UDN environment, the probability for the desired and

interfering signals of experiencing different loss levels is quite high, resulting in dissimilar path loss exponents. Furthermore, the probability of a link within a reference distance, e.g. $d \in (0, 1)$, becomes high, and thus this phenomenon cannot be neglected in the analysis. Consequently, a widely accepted unbounded single-slope path loss model, i.e., $G(d) = d^{-\alpha}$, becomes dubious in a UDN. With this regard, research in bounded multi-slope path loss models becomes necessary in such scenarios. Moreover, a non-negligible portion of BSs become inactive without interfering other cells in a UDN (Fig. 1.2). In this case, a full load model where BSs always transmit signals will overestimate the interference level.

A multi-slope path loss model is applied in [26] (step (d)), which shows that UE coverage probability is a decreasing function of BS density under such modeling. Meanwhile, [27] investigates the effect of bounded path loss model when BS density is extremely large (step (c)). Both [26] and [27] provide vanishing SIR as BS density grows asymptotically. On the contrary, the conclusions of [28] and [29] indicates that SIR keeps increasing as BS density goes to infinity (step (b)). Such contradiction comes from the corresponding models in the references. The bounded and multi-slope path loss models help to prevent overestimating the signal power and underestimating the interference respectively, which decrease the SIR. Conversely, the partial load model can prevent overestimating the interference density in the whole network, which increases the SIR. Therefore, it is interesting and necessary to understand the real asymptotic behavior of ultra densification by incorporating all the factors (step (e)).

1.3 Thesis Focus and Problem Formulation

Based on the literature review, there is a general agreement on the effectiveness and powerfulness of network densification. It has been recognized as the single most effective way to increase network capacity [30]. This is because the capacity scales linearly with the BS density as long as power-law path loss models (single-slope models) hold and every BS serves at least a single UE [31]. According to such 'theory', keep densifying endlessly, problem solved. Regardless of the impractical backhauling problems, *is this true*? This rises the first high-level research question (HQ) that we try to answer in this thesis:

- HQ 1: *How dense should the network be?*

The enormous capacity increase is composed by various types of traffic demands, e.g., extreme high data rates or massive device connections. Given the three factors in Fig. 1.1, mobile network operators (MNO) need to make a decision on which direction to head to, for the purpose of meeting the certain traffic demand efficiently. To this end, we will focus on the competence of network densification towards the other two elements (spectrum and multi-antennas) in answering HQ1. Thus, the following research questions (RQ) should be addressed:

- RQ 1: *What is the trade-off between densification and other resources in order to fullfill certain requirement?*

- RQ 2: *What kind of traffic demand is better served by network densification?*

Recently, the well-known Moore's Law has hit a plateau, resulting in wide ranging ramifications beyond the semiconductor industry. The analogous Cooper's Law may face the similar problem sooner or later. As discussed previously, the conclusion of linearly increased capacity are drawn under very simple load and propagation assumptions. In this case, the gain of network densification may be exaggerated. Therefore, a clear understanding of the asymptotic behavior of ultra-densification incorporating more realistic load and propagation models is needed. With this regard, we aim to answer the following research question:

- RQ 3: *What is the fundamental limits of ultra-densification?*

The existing UDN studies mainly focus on single BS association. The BSs without UE in their coverage area are considered in sleep mode and not transmit any signals. In extreme cases, a huge number of dormant BSs will temporarily stay idle in the network. Viewed from one angle, the dormant BSs can save energy and reduce interference. But seeing from another angle, the dormant ones may potentially provide capacity gain to the active UEs. Thus, it raises the second high level research question in this thesis:

- HQ 2: *How can we exploit the temporary infrastructure 'redundencies' in UDN to improve the system performance?*

Joint transmission (JT) which allows multiple BSs jointly serve one UE, is a potential approach. By applying JT, the dominant interferences could be turned into useful signals while the other interferences remain the same in traditional fully loaded cellular networks [32]. Thus, the desired signal strength increases and interference decreases concurrently so that the UE will get higher signal-to-interference ratio (SIR). However, interference nature in a UDN is essentially different from that in a traditional network. The reason is that turning on dormant BSs in a UDN will both improve the desired received signal strength to a certain UE and generate extra interference to other cells. Therefore, the following two questions need to be addressed:

- RQ 4: *How to design cooperation schemes in UDN in order to improve individual UE rate?*

- RQ 5: *Under which conditions is cooperation preferable in a UDN?*

1.4 Overview of Thesis Contributions

This section summarizes the main contributions of the thesis. To put our work into the context of current research, an overview of the thesis contribution is listed as follow:

Chapter 3

In this chapter, we study the resource trade-offs in network provisioning. In spite of abundant research in each of the three ingredients aforementioned, there has been little knowledge on the relationship among them. Respecting the uncertainty, we introduce microeconomic terminology 'technical rate of substitution' (TRS) to illustrate the value of densification in terms of spectrum and antenna number per BS. The substitutability of densification is discussed by calculating the TRS between BS density and other elements in different scenarios. Furthermore, we also demonstrate the importance of specifying demand types in the dimensioning of wireless networks. We show that different resources are needed in different traffic demand types even with the same area throughput. Our study can give an insight to operators on the proper choice of resources to allocate for purposes in different scenarios. This chapter is based on the following papers:

- **Paper I**. Y. Yang and K. W. Sung, "Tradeoff between Spectrum and Densification for Achieving Target User Throughput," in Vehicular Technology Conference (VTC Spring), 2015 IEEE 81st, May 2015.

- **Paper II**. Y. Yang and K. W. Sung, "Technical Rate of Substitution of Spectrum in Future Mobile Broadband Provisioning," in Dynamic Spectrum Access Networks (DySPAN), 2015 IEEE International Symposium on, October 2015 (Best poster award).

- **Paper III**. A. Widaa, Y. Yang, K. W. Sung and J. Markendahl, "On the Engineering Value of Spectrum in Dense Mobile Network Deployment Scenarios" in Dynamic Spectrum Access Networks (DySPAN), 2015 IEEE International Symposium on, October 2015.

The author of this thesis acted as the main author of Paper I and Paper II and developed the simulation methodologies. The problem formulations are jointly proposed with Dr. Ki Won Sung. The author of the thesis acknowledges Dr. Anders Furuskär at Ericsson Research for his valuable suggestions and feedback. In Paper III, the author of this thesis has contributed the analytical models and proofreading.

Chapter 4

The Asymptotic Behavior of Ultra-Densification is studied in this chapter. To the best of our knowledge, this is the first UDN work combining both the effect of UE density and a multi-slope path loss model. We discuss the convergence of the asymptotic behaviors depending on different load situations. Numerically tractable integral-expression as well as closed-form bounds of coverage probability and ASE are derived. Furthermore, the impact of UE density on coverage probability and ASE are analyzed. This chapter is based on the following paper:

- **Paper IV**. Y. Yang, J. Park. and K. W. Sung, "On the asymptotic behavior of ultra-densification under a bounded dual-slope path loss model," Submitted to IEEE ICC 2017.

The author of the thesis proposed the original problem, provided the deriviations and acted as the leading author of the paper. Dr. Jihong Park made contributions by refining the structure and polishing the writing of the paper. Dr. Ki Won Sung provided directions and valuable insights in the paper.

Chapter 5

This chapter intends to give a first look at applying BS cooperation in a partially loaded UDN scenario. Similar with the previous chapter, a bounded dual-slope path loss model is employed to capture the characteristics of UDN. We investigate two BS cooperation schemes: non-coherent JT without the assistance of instantaneous channel state information (CSI) and coherent JT with full CSI knowledge. Meanwhile, the effect of imperfect CSI on cooperation gain is discussed. Finally, we categorize the conditions which are favorable for JT in a UDN environment. This chapter is based on the following paper:

- **Paper V**. Y. Yang, K. W. Sung, J. Park S. L. Kim and K. Kim, "Cooperative transmissions in ultra dense networks under a bounded dual-slope path loss model," Submitted to IEEE ICC workshop 2017.

The author of this thesis proposed the original problem formulation, implemented the simulation methodologies and acted as the leading author. Dr. Jihong Park and Dr. Ki Won Sung offered valuable feedbacks on writing and the structure of the paper. Prof. Seong-Lyun Kim and Prof. Kwang Soon Kim provided comments on the problem formulation.

1.5 Thesis Outline

The remainder of the thesis is organized in two parts: an over view of the thesis (Chapter 2 to 6) and verbatim copies of the papers includes in this thesis. In Part I, Chapter 2 introduces the stochastic geometry based model and methodology

employed in this thesis. The key results of the thesis are present from Chapter 3 to 5. Finally, the concluding remarks and future work are discussed in Chapter 6.

Chapter 2

Modeling and Methodology

In this chapter, we first introduce the background of wireless network modeling and our motivation to utilizing stochastic geometry framework as our methodology. Then, further details on theoretical models in this thesis are present. At last, we discuss the pros and cons of such approach.

2.1 Introduction

A wireless communication network can be viewed as a collection of points, which can in turn represent transmitters or receivers. Accurate models are essential to the development of standards and the evaluation of system performance or potential schemes in wireless networks. The most widely used and accepted model is the hexagonal grid model. It is frequently used in system-level simulations but is not generally possible for analytical study [33] [34]. With the grid model, tractable analysis can only be achieved for some fixed-location UEs, e.g., cell corner. Such an approach cannot provide information on the performance of the most UEs in the system. A popular analytical model for multi-cell systems is the Wyner model [35]. It assumes a unit gain from each BS to its serving UE and equal channel gains to the two neighboring UEs in a one-dimensional space. In this case, the SINR for all UEs are deterministic and thus one cannot distinguish between cell edge and interior UEs. Such a model is reasonable in a system where other-cell interference is approximated to a constant, such as the code division multiple access (CDMA) uplink, but it is highly inaccurate in general and particularly for systems with 1 or 2 dominant interferers, like an orthogonal frequency-division multiple access (OFDMA) based 4G and beyond network [36]. Recently, a prominent approach has drawn attentions in academia, which uses random spatial models from stochastic geometry to capture the real deployment. Such approach is rapidly gaining momentum due to its great analytical tractability.

Stochastic Geometry is the theory of random sets, which forms random processes of points, particles, fibres or surfaces in the Euclidean space. It is widely used

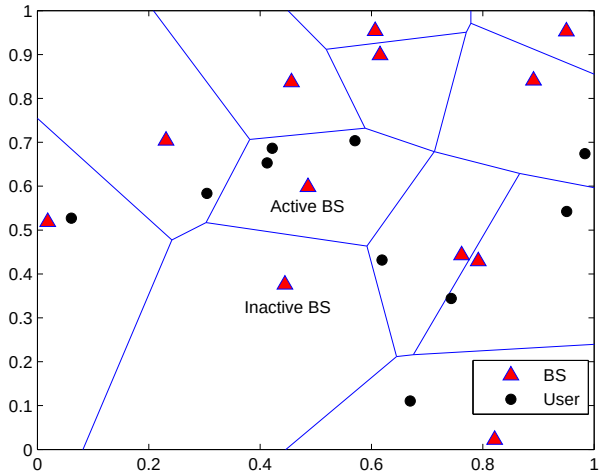

Figure 2.1: Network topology based on the PPP assumption

to model complicated geometrical patterns, which occur in many areas of science and technology. Examples include the structures studied in geology, sections of porous media, solid bodies, biological tissues, and patterns formed by the distinction between wood and field in a landscape [37]. Modeling communication networks with stochastic geometry is relatively new. One can consider Gilbert's paper of 1961 [38] as the first paper on the analysis of the connectivity of large wireless networks by means of stochastic geometry. The engineering literatures appeared shortly before 2000 [39] [40]. Since then, the number of papers using stochastic geometry based models is increasing fast and becoming even faster recently thanks to its capability of well-matching the emerging small cell/heterogeneous networks [31].

2.2 Network modeling with stochastic geometry

In stochastic geometry analysis, the network is abstracted to a point process (PP) to model the positions of the network entities according to the network type and/or the MAC layer behavior. The most popular PPs include Poisson point process (PPP), hard core point process (HCPP), Poisson cluster process (PCP) and etc. Among these PPs, the PPP is the most popular because the assumption of independent BS locations allows substantial tools from stochastic geometry and provides tractable analysis. The accuracy of the PPP model is validated by comparing with the grid model and an actual 4G network [25].

In a downlink cellular network, the BSs and UEs are modeled to be distributed according to two independent homogeneous PPPs, Φ_b and Φ_u. The densities of

BS and UE are denoted as λ_b and λ_u respectively. The coverage area of each BS comprises a Voronoi tessellation as shown in Fig. 2.1. We assume closest association rule, i.e., the UEs in the Voronoi cell of a BS are served by it. As BS density increases, some BSs may not contain any active UEs in its coverage area. In this case, the BS becomes inactive without transmitting any signal. Each active BS has at least one UE in its cell and will randomly choose one of them to serve. The probability of a BS being active is derived in [41], given as:

$$p_a = 1 - (1 + \frac{\lambda_u}{3.5\lambda_b})^{-3.5}. \tag{2.1}$$

The standard propagation model $\ell(d) = d^{-\alpha}$ is considered with path loss exponent $\alpha > 2$, unless otherwise stated (e.g. Chapter 4). Both BS and UE are equipped with single antenna and BS transmits with unit power unless otherwise noted (e.g. Chapter 3). Rayleigh fading is used to model the channel gain, with the fading coefficients h are i.i.d zero mean unit variance complex normal distributed random variables. Shadow fading is ignored for brevity and it is shown to not significantly affect the accuracy of the analysis [25, 42].

Without loss of generality, we conduct analysis on the performance of a typical UE located at the origin o and randomly selected by its serving BS, which is permissible in a homogeneous PPP according to Slivnyak's theorem [43]. As we are dealing with UDN scenario where BS-UE distance is quite close in the thesis, it is reasonable to assume an interference-limited system. Thus, we will neglect the noise power and examine signal-to-interference-ratio (SIR) instead of SINR throughout the thesis. Such assumption is justified through simulation in [24, 42]. The SIR of the typical UE denoted as 0 can be expressed as

$$\mathrm{SIR}_0 = \frac{|h_{0,0}|^2 \ell(d_{0,0})}{\sum\limits_{i \in \Phi_b^* \setminus 0} |h_{i,0}|^2 \ell(d_{i,0})}. \tag{2.2}$$

where $h_{i,j}$ and $d_{i,j}$ denote the channel and distance between BS i and UE j respectively, $|h_{i,j}|^2 \sim \exp(1)$. Φ_b^* represents the set of active BSs which is not a homogeneous PPP because the active probability depends on the cell area. Nevertheless, we can model Φ_b^* as a homogeneous PPP with density $\lambda_b^* = \lambda_b p_a$, by thinning the process Φ_b. This approximation has been shown to be accurate according to [42, 44].

Given the downlink SIR of the typical UE, the coverage probability is defined as:

$$P_c(\lambda_b, \lambda_u, T) \triangleq \mathbb{P}[\mathrm{SIR}_0 > T] \tag{2.3}$$

where T is the target SIR level.

The network ASE Γ is given by

$$\Gamma(\lambda_b, \lambda_u, T) \triangleq p_a \lambda_b P_c(\lambda_b, \lambda_u, T) \log_2(1+T) \tag{2.4}$$

where $p_a \lambda_b P_c$ can be interpreted as the density of the BSs that successfully transmit the symbols to their UEs.

2.3 Pros and cons of stochastic geometry approach

Stochastic geometry is a powerful mathematical technique available that provides a rigorous analytical approach to the modeling, analysis, and design of heterogeneous cellular networks [45]. By modeling the networks as PPPs with Rayleigh fading, one can obtain short closed-form expressions with high tractability. Such baseline provided by stochastic geometry modeling can help understanding the effects of the fundamental design parameters on the system behavior.

The major drawback of stochastic geometry modeling is the limitation of spatial averaging. Considering only spatial averages may hide important details that affect the network performance. It will limit the insights that can be obtained and the effect of the design parameters due to the spatial randomness [46]. For instance, it is hard to capture the performance of cell edge or lower 5 percentile UEs. Accordingly, we cannot design the network where at least 95% of the UEs experience an outage probability less than 5% only with the spatial average of the outage probability. Thus, a combination of using different tools is necessary for different purposes of analysis.

Chapter 3

Resource Trade-offs in Network Provisioning

In order to quantify the resource requirement in UDN in terms of BS density, antenna numbers and spectrum, we need to figure out the relationships among them. Besides, resource requirement depends on the traffic demand. Area capacity is widely used for describing demand target in previous works. However, it hardly captures the individual UE requirement which is a key performance indicator in 5G or beyond [47]. Same area capacity may result in various types of traffic demand that need different amount of resources. Therefore specifying demand types can help operators allocating resources properly. In this chapter, we study the relations among the three elements under different types of traffic demand. The details of the analysis and more results can be found in Paper I II and III.

3.1 System model

In this chapter, we assume a multi-input-single-output (MISO) system, i.e., each BS has M antennas while each UE is equipped with a single antenna. Maximal ratio transmission (MRT) beamforming is chosen for multi-antenna technique and the precoder is designed as $w_i = \frac{\mathbf{h}_{ii}^*}{\|\mathbf{h}_{ii}\|}$ where $\mathbf{h}_{i,j} \sim \mathcal{CN}(0, \mathbf{I})$ is a $M \times 1$ vector denoting the MISO channel. Thus, the SIR of the typical UE 0 can be expressed as

$$\mathrm{SIR}_0 = \frac{g_{0,0}\ell(d_{0,0})}{\sum\limits_{i \in \Phi_b^* \setminus 0} g_{i,0}\ell(d_{i,0})}. \tag{3.1}$$

where $g_{0,0} = \| \mathbf{h}_{00} \|^2 \sim$ Gamma$(M, 1)$ and $g_{i,0} = \frac{\|\mathbf{h}_{ii}^* \mathbf{h}_{ii}\|^2}{\|\mathbf{h}_{ii}\|^2} \sim$ Exp(1) for $i \neq 0$ [48], the path loss exponent α is set to 4.

Given the SIR, the coverage probability is derived in [42] as

$$P_c = \frac{1}{p_a} \left\| \left[\left(k_0 + \frac{1}{p_a} \right) \mathbf{I} - \mathbf{Q}_M \right]^{-1} \right\|_1 \tag{3.2}$$

where $\| \cdot \|_1$ is the L_1 induced matrix norm, $\mathbf{I}$ is an $M \times M$ identity matrix, $\mathbf{Q}_M$ is an $M \times M$ Toeplitz matrix given by

$$\mathbf{Q}_M = \begin{pmatrix} 0 & & & & \\ k_1 & 0 & & & \\ k_2 & k_1 & 0 & & \\ \vdots & & & \ddots & \\ k_{M-1} & k_{M-2} & \cdots & k_1 & 0 \end{pmatrix} \tag{3.3}$$

$k_0 = \frac{\frac{2}{\alpha}T}{1-\frac{2}{\alpha}} {}_2F_1(1, 1-\frac{2}{\alpha}; 2-\frac{2}{\alpha}, -T)$, and $k_i = \frac{\frac{2}{\alpha}T^i}{i-\frac{2}{\alpha}} {}_2F_1(i+1, i-\frac{2}{\alpha}; i+1-\frac{2}{\alpha}, -T)$ for $i \geq 1$, where ${}_2F_1(\cdot)$ is the Gauss hypergeometric function.

In this chapter, we choose typical UE data rate as our performance metric. It is defined as the average downlink ergodic rate of a typical UE in the network, denoted as R_a. R_a can be expressed as a function of P_c and is given by

$$\begin{aligned} R_a &= W\mathbb{E}[\log_2(1 + \text{SIR})] \\ &= \frac{W}{\ln 2} \int_{T>0} \frac{P_c}{T+1} dT \end{aligned} \tag{3.4}$$

3.2 Technical Rate of Substitution

The concept from microeconomics, TRS, is introduced to explain the value of network densification. TRS measures the rate at which the firm will have to substitute one input for another in order to keep output constant. Suppose that we have factors, e.g. spectrum and BS density, and are operating at some point (W, λ_b) with output of data rate R_a. Consider a change in W and λ_b while R_a keeps fixed:

$$R_a = f(\lambda_b, W) = f(\lambda_b + \triangle\lambda_b, W + \triangle W). \tag{3.5}$$

Then the TRS of λ_b with regard to W at point (λ_b, W) is defined as

$$\mathbf{TRS}(\lambda_b, W) = \left| \frac{\triangle W}{\triangle \lambda_b} \right| \tag{3.6}$$

which indicates the substitutability of BS density. If the TRS of λ_b is low, it means BS can be easily replaced by acquiring more spectrum. Otherwise, deploying more BSs is more effective.

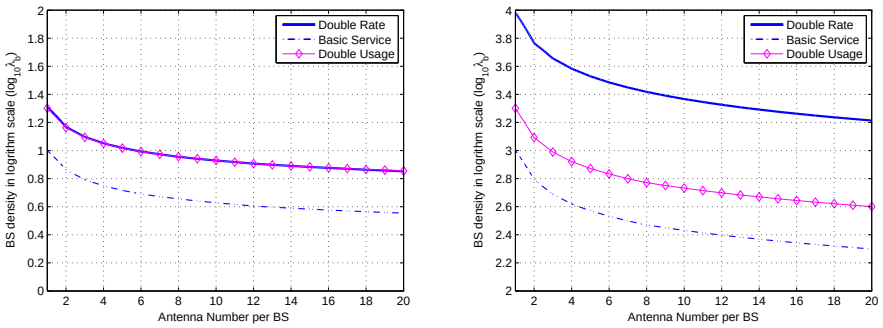

(a) Sparse network (b) Dense network

Figure 3.1: Relation between antenna number and BS density. (©2015 IEEE.)

Table 3.1: TRS between antenna number and densification ($\frac{\triangle M}{\triangle \lambda_b}$). (©2015 IEEE.)

Sparse Case	M=1	M=4	M=8	M=16
λ_u=100 R_a=15Mbps	0.374	2.664	5.739	23.244
Dense Case	M=1	M=4	M=8	M=16
λ_u=100 R_a=420Mbps	0.0026	0.022	0.075	0.154

We will evaluate the relations among BS density λ_b, spectrum bandwidth W and antenna number per BS M. Our objective is to calculate $\mathbf{TRS}(\lambda_b, W)$ and $\mathbf{TRS}(\lambda_b, M)$ at each operating point of basic service. Beyond that, we consider increasing the network capacity from either speed or usage perspective and investigate the resource requirement for the two network upgrading purposes.

3.3 Key results

We consider two scenarios: sparse network representing the current deployment and dense network for the future. Sparse and dense are interpreted by the relative BS-UE density ratio $\rho = \frac{\lambda_b}{\lambda_u}$. We choose $\rho = 0.1$ and $\rho = 10$ for sparse and dense scenario respectively while λ_u is fixed to 100 per area. The resource requirement for two purposes are investigated: increasing the individual UE data rate or accommodating more active UEs, which constitute the same area capacity increase.

3.3.1 TRS of densification

Figure 3.1 depicts the relationship between BS density and antenna number. The indifference curves represent resource combinations that can fulfill the same traffic

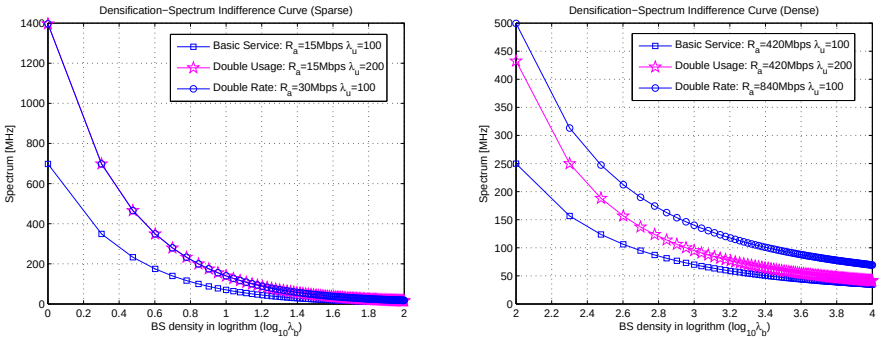

(a) sparse (b) dense

Figure 3.2: Relation between spectrum and BS density. (©2015 IEEE.)

Table 3.2: TRS between spectrum and densification ($\frac{\triangle \text{MHz}}{\triangle \lambda_b}$). (©2015 IEEE.)

Sparse Case	λ_b=1	λ_b=5	λ_b=10
λ_u=100 R_a=15Mbps	349.650	23.256	6.289
Dense Case	λ_b=100	λ_b=500	λ_b=1000
λ_u=100 R_a=420Mbps	2.398	0.080	0.030

demand. For basic service, adding antenna number has a diminishing gain in terms of BS density which is also reflected in the growing TRS in Table 3.1. Meanwhile, multi-antenna performs better in dense networks according to the small TRS values.

The spectrum-densification trade-offs are illustrated in Fig. 3.2 and Table 3.2. In sparse region, the slope of the curve is sharp which indicates densification can save large amount of spectrum. When it comes to dense network, only a portion of BSs are active since BSs outnumber UEs. Therefore, a further densification will add even more idle BSs which is not effective, though slightly helpful, for the throughput increase. Similar with installing antennas, investing spectrum is more effective in dense network as well (with smaller TRS).

3.3.2 Impact of traffic types

In Figs. 3.1 and 3.2, we also present the resource requirement for 2 times more area capacity but with different traffic types. In sparse network, the coincident indifference curves demonstrate that doubling data rate and doubling usage requires same amount of resource. Meanwhile, BS density and spectrum are linearly exchangeable in this region, i.e., either 2x spectrum or 2x densification can accomplish 2x capacity requirement. Nevertheless, in dense network, twofold densification can still

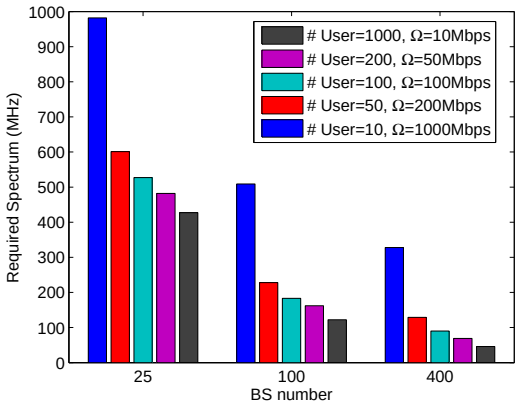

Figure 3.3: Resource requirement in different traffic demands. (©2015 IEEE.)

achieve double usage but is far apart from meeting double data rate requirement. This phenomenon is further explained in Fig. 3.3 in which five traffic types with the same area throughput are compared. It is shown that densification plays a more important role in accommodating massive UEs while spectrum has a significant impact in the bursty situation.

3.4 Summary

In this chapter, by studying the TRS, we measure the relative effectiveness of network densification over acquiring spectrum or installing multiple antennas on BSs. The high TRS indicates that network densification is the key solution to capacity increment in sparse network. Spectrum and multi-antenna[1] can have additional merits especially in dense networks. We also demonstrate the importance of specifying user demand in network dimensioning by showing that the resource requirement in different traffic demand types with the same area throughput. It is observed that increasing data rate of individual users requires more resources than accommodating more usage.

[1] Only MRT beamforming is evaluated, zero forcing or other schemes may have different results.

Chapter 4

Asymptotic Behavior of Densification

In the previous chapter, we observe a diminishing impact of densification as BS density keeps increasing. However, the end point of densification is not foreseeable from there. In this chapter, we present our results on the asymptotic behavior of ultra-densification. In a UDN environment where cell sizes are much smaller, the single-slope standard path loss model becomes too idealized. It is important to capture the propagation characteristics of a UDN for providing accurate results. With this regard, a bounded dual-slope path loss model is considered in our UDN analysis. We demonstrate the convergence of coverage probability of a typical UE in asymptotic regions. The impact of UE density on coverage probability and ASE is emphasized as well. The details of the analysis and more results can be found in Paper IV.

4.1 Bounded dual-slope path loss model

We consider that path loss attenuation from a BS to a UE is distinguished under three different regions, *bounded* region, *near-field* and *far-field* at the UE as illustrated in Fig. 4.1. Bounded region is a closed circle centered at the UE, inside which the path loss is assumed to be constant (e.g. 1). The radius of the circle is always no smaller than 1 so that the transmitted signal power cannot be amplified at the receiver side. The *near-field* and *far-field* are regions of the electromagnetic field around an object. For antennas shorter than half of the wavelength of the radiation they emit (i.e., "electromagnetically short" antennas), the near and far regional boundaries are measured in terms of a simple ratio of the distance r from the radiating source to the wavelength λ of the radiation. For antennas physically larger than a half-wavelength of the radiation they emit, the near and far fields are defined in terms of the Fraunhofer distance $R_F = \frac{2D^2}{\lambda}$ where D is the antenna size [49]. In this thesis, our definition is similar with the latter as in other refer-

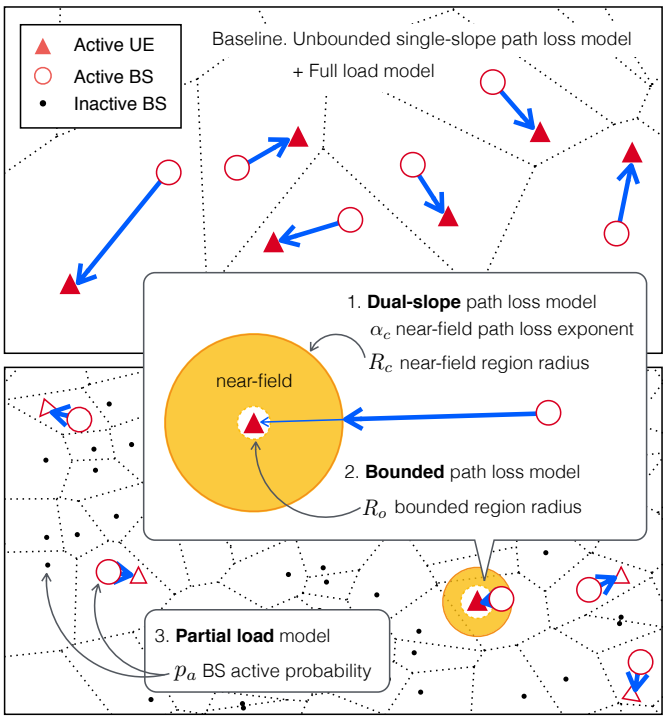

Figure 4.1: A bounded dual-slope path loss model

ence [26]. *Near-field* consists of reactive and radiative regions, wherein a proportion of inductive or capacitive energy is stored near the antenna surface. Hence, signal power decays slowly within this region. In *far-field*, the signal experiences more absorption and diffraction which makes larger path loss exponents in *far-field* than in *near-field* regions.

The bounded dual-slope path loss model can be formulated in a piece-wise function of the transmission distance d, shown as

$$\ell(\alpha_1, \alpha_2, d) = \begin{cases} 1, & 0 \le d \le R_b; \\ d^{-\alpha_c}, & R_b < d \le R_c; \\ \tau d^{-\alpha}, & d > R_c \end{cases} \tag{4.1}$$

where $R_b > 0$ is the radius of bounded path loss region, i.e., the path loss in the range of $[0, R_b]$ is assumed constant; $\tau \triangleq {R_c}^{\alpha-\alpha_c}$ which keeps the continuity of the function; $R_c \ge R_b$ is the critical distance to divide the *near-* and *far-field*; and α_c and α are the *near-* and *far-field* path loss exponents for $2 \le \alpha_c \le \alpha$, respectively.

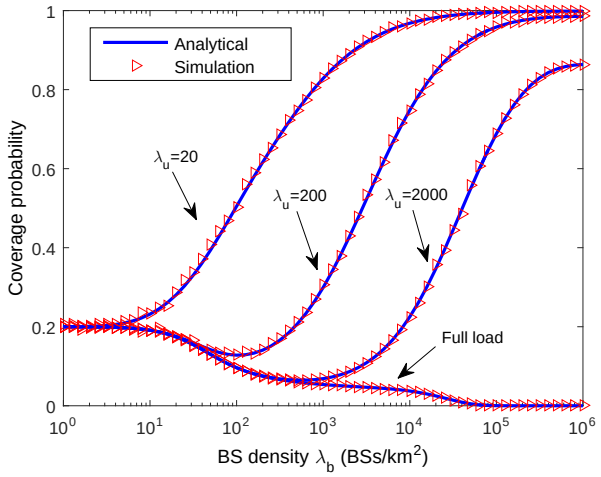

Figure 4.2: Effect of λ_u on coverage probability under bounded dual-slope model.

4.2 Key results

By incorporating the bounded dual-slope propagation and partial load model ((2.1) in Chapter 2), the exact form of coverage probability along with its upper and lower bounds is derived in Paper IV. Based on the bounds, we further show the convergence of the coverage probability and ASE in asymptotic regions: As $\lambda_b \to \infty$, SIR coverage probability and ASE converge to finite values as follows:

$$\lim_{\lambda_b \to \infty} P_c(\lambda_b, \lambda_u, T) = e^{-\lambda_u \pi c_T(\alpha, \alpha_c, R_c, R_b)} \tag{4.2}$$

$$\lim_{\lambda_b \to \infty} \Gamma(\lambda_b, \lambda_u, T) = \lambda_u e^{-\lambda_u \pi c_T(\alpha, \alpha_c, R_c, R_b)} \log_2(1+T) \tag{4.3}$$

where $c_T(\alpha, \alpha_c, R_c, x) := {R_c}^2 F\left(\frac{2}{\alpha}, \frac{1}{T}\left[\frac{R_c}{x}\right]^\alpha\right) - {R_b}^2\left[F\left(\frac{2}{\alpha}, \frac{1}{T}\right) - \frac{T}{1+T}\right] + \frac{2T{R_b}^\alpha {R_c}^{2-\alpha}}{\alpha_c - 2} F\left(1 - \frac{2}{\alpha_c}, T\left[\frac{x}{R_c}\right]^\alpha\right)$ and $F(b,z) = {}_2F_1(1, b, 1+b, -z)$ with ${}_2F_1(a,b,c,z)$ being the Gauss hypergeometric function.

Monte Carlo simulations are implemented to validate our theoretical analysis. In the simulation, we set $R_b = 1m$, $R_c = 70m$, $\alpha_c = 2.5$, $\alpha = 4$ and the SIR threshold T = 10dB in all of our results. To calculate or simulate 'fully loaded network', we set $\lambda_u = 2 \times 10^8/\text{km}^2$ which is a sufficiently large value so that $p_a \approx 1$.

The effect of UE density on coverage probability is illustrated in Fig. 4.2 where our analysis and simulations are well-matched. Meanwhile, we find that coverage

probabilities show completely different trends among different UE densities. In full load model, the coverage probability starts to decline when the BS density is sufficiently large so that there are interfering BSs inside the *near-field* of the typical UE. It will keep decreasing towards zero as BS density grows. When λ_u is high but finite (e.g. $\lambda_u = 200$ or 2000), all the UEs will get served as BS density increases and the interference becomes saturated. Thus the coverage probability will first decrease and start increasing again after the saturation. In contrast, when UE density is low (e.g. $\lambda_u = 20$), the probability of no interferer inside the *near-field* of the typical UE is very high. Hence, the coverage probability becomes a non-decreasing function of λ_b. Meanwhile, we find that the converged value of the coverage probability will decrease as UE density grows and decay to zero in the full load case. The reason is that the desired signal is restricted by the bound effect in asymptotic regions and the overall performance will depend on the interference which refers to UE density.

Figure 4.3 depicts the scaling of ASE with regard to BS density. We observe that the ASE first increase with BS density and then converge to a constant which aligns with our theoretical analysis. The constant is larger than 0 in partially loaded network and becomes 0 when the network is full load ($\lambda_u \to \infty$). Also, the performance is overestimated with unbounded or single-slope models in ultra-dense regions. This is because the simplified models either exaggerate the desired power inside the bounded region or underestimate the interference in the *near-field*. By comparing Fig. 4.3 with Fig. 4.2, we find that a trade-off occurs between UE coverage probability (reliability) and network ASE (rate) during BS densification. In full load case, network ASE keeps increasing before $\lambda_b = 10^4$ despite the declining coverage probability. For partially loaded network with $\lambda_u = 200$, the trade-off exists approximately between $\lambda_b = 10^{1.5}$ to $\lambda_b = 10^3$.

4.3 Summary

In this chapter, we investigate the asymptotic behavior of ultra-densification of base stations. With more sorphisticated propagation and load models, we find that the asymptotic behavior of ultra-densification is different from what was known with simpler assumptions. Both UE coverage probability and ASE converge to a non-zero value unless the UE density goes to infinity. Our results also suggest that the densification cannot always improve the individual UE performance or boost the network throughput.

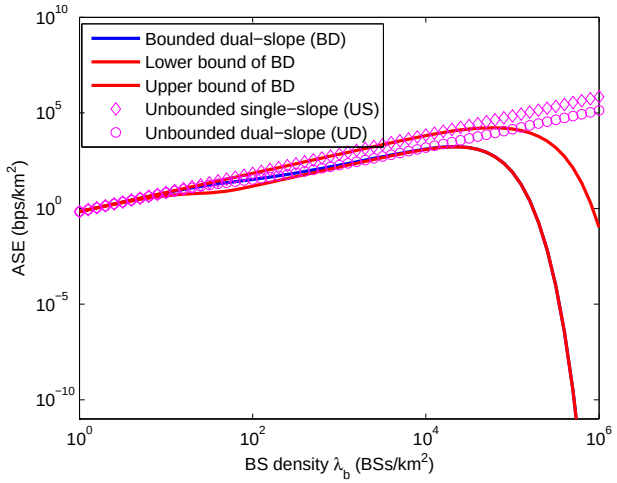

(a) ASE when network is fully loaded

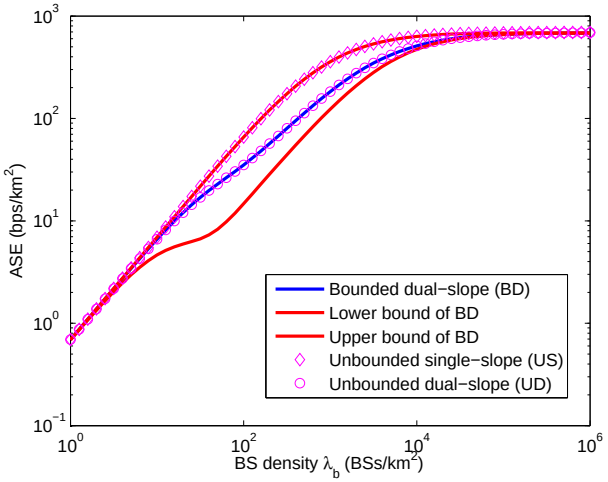

(b) ASE when $\lambda_u = 200$

Figure 4.3: ASE bounds and comparison with previous models.

Chapter 5

Cooperative transmissions in UDN

In a UDN, it is possible that many BSs are instantaneously left idle. With this regard, it will be beneficial if we can utilize the idle BSs properly to provide capacity gains. Joint transmission from several BSs to one UE is one potential candidate in this scenario. However, JT in a UDN is fundamentally different from in a traditional full load network. Thus, how to design JT in a UDN is of our concern. In this chapter, we will investigate the performance of two types of cooperation schemes in a UDN: non-coherent JT without CSI and coherent JT with full CSI knowledge. Similar with that in Chpater 4, a bounded dual-slope propagation model and partially loaded network are considered. Meanwhile, the impact of different environmental parameters such as critical distance and path loss exponents on cooperation schemes are discussed. More details and results can be found in Paper V.

5.1 System model

In previous studies, e.g., [18] [41], the network topology is composed by BS-centric Voronoi cells which represent the BS coverage areas as shown in Fig. 2.1. However, since there exists massive empty cells in a UDN, BS-centric topology may lead to an ineffective map partition. Concerning this, we propose to reverse the roles of BS and UE in the topology and utilize UE-centric Voronoi cells for modeling the cooperation in a UDN, as shown in Fig. 5.1. The BSs inside a UE-centric Voronoi cell is closer to the particular UE than to other UEs. Moreover, based on the UDN density assumption, we can approximate the kth closest BS inside the Voronoi cell as the kth closest BS in the entire network when $k \ll \frac{\lambda_b}{\lambda_u}$.

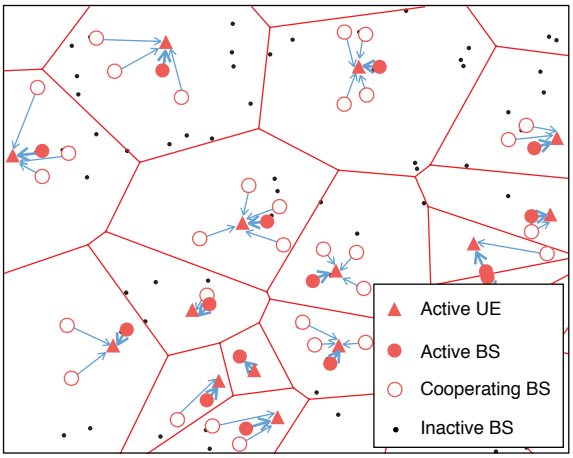

Figure 5.1: UE-centric Voronoi cells for modeling cooperative transmissions in a UDN.

5.2 Cooperative transmission models

5.2.1 Cooperation schemes

We assume any UE i in the network is jointly served by the set of N closest BSs in its own Voronoi cell, denoted by $\mathcal{C}_i = \bigcup_{j=1}^{N} BS_j$. Within the cooperation set, all BSs jointly transmit the same message to the UE using the same frequency band. We denote $\Phi_{\mathcal{C}}$ as the set of active BSs in the whole network.

In non-coherent JT, the receivers apply open-loop joint processing scheme as in [50], where signals from different transmitters are added by power summation. The desired signal power for non-coherent JT is given by

$$\mathcal{S}_i^{NJ} = \sum_{x \in \mathcal{C}_i} |h_{x,i}|^2 \ell(d_{x,i}) \tag{5.1}$$

where $d_{x,i}$ and $h_{x,i}$ denote the distance and channel between BS x and UE i, $h_{x,i} \sim \mathcal{CN}(0,1)$.

In coherent JT, we assume the CSI is available at the BS side. In this case, BSs can design precoder to adjust the phase shift of the channel and amplify the corresponding channel gain. Similar with that in Chapter 3, we employ MRT precoder such that $w_x = \frac{h_x^*}{|h_x|}$. The desired signal power for coherent JT is thus

$$\mathcal{S}_i^{CJ} = \left| \sum_{x \in \mathcal{C}_i} h_{x,i} w_{x,i} \sqrt{\ell(d_{x,i})} \right|^2 . \tag{5.2}$$

Therefore, the SIR of UE i with two cooperation schemes, γ_i^{NJ} and γ_i^{CJ} are shown as follows:

$$\gamma_i^{NJ} = \frac{\mathcal{S}_i^{NJ}}{\sum\limits_{x \in \Phi_{\mathcal{C}} \setminus \mathcal{C}_i} |h_{x,i}|^2 \ell(d_{x,i})} \tag{5.3}$$

$$\gamma_i^{CJ} = \frac{\mathcal{S}_i^{CJ}}{\sum\limits_{x \in \Phi_{\mathcal{C}} \setminus \mathcal{C}_i} |h_{x,i}|^2 \ell(d_{x,i}).} \tag{5.4}$$

5.2.2 Cooperation Gains

The UE SE $\mathcal{R}$ is chosen as the performance metrics. The SE derived by the Shannon formula is given by

$$\mathcal{R} = \log_2(1 + \gamma). \tag{5.5}$$

We set the UE SE under single association $\mathcal{R}^o$ as our baseline to measure the gain of cooperation. The SE gain G_c is defined as the ratio between SE difference $\Delta_{\mathcal{R}}$ and $\mathcal{R}^o$ as follows:

$$G_c = \frac{\Delta_{\mathcal{R}}}{\mathcal{R}^o} = \frac{\mathcal{R}^J - \mathcal{R}^o}{\mathcal{R}^o} \tag{5.6}$$

where $\mathcal{R}^J$ and $\mathcal{R}^o$ are the SE with and without cooperation, respectively.

5.3 Key results

We first present the performance of both cooperation schemes in terms of critical distance in Fig. 5.2. To our surprise, non-coherent JT has even worse performance than single BS association. In non-coherent JT, the desired power summation grows diminishingly because the transmitting distance gets longer, but the interference can be considered as almost linearly increasing with the number of cooperating BSs [24]. As a result, the increment in the desired signal cannot compensate the faster growing interference which leads to no gain. Thus, we will neglect non-coherent JT in further discussions. Regarding coherent JT, we find that the cooperation gain grows along with critical distance. When critical distance is short, more cooperating BSs make SE even worse; when the critical distance is large, the cooperation gain increases with the number of cooperating BS.

Fig. 5.3 depicts the impact of different dual-slope path loss exponents. The cooperation gain decreases with both *near-field* and *far-field* path loss exponents. Since the SE is an increasing function of path loss exponent without cooperation, a smaller exponent will lead to a lower baseline of performance and/or an improvement in the near-field JT signal, thereby providing a better cooperation gain.

The impact of active UE and BS densities on cooperation is shown in Fig. 5.4 and Fig. 5.5. First, as active UE density increases, cooperation gain keeps growing while SE drops because the baseline gets lower and more interference is generated.

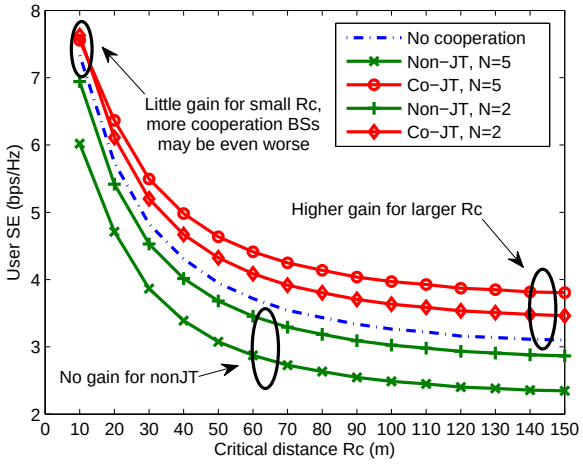

Figure 5.2: User performance with different critical distances when path loss exponents=[2,4], $\lambda_b = 4000/\text{km}^2$, $\lambda_u = 200/\text{km}^2$.

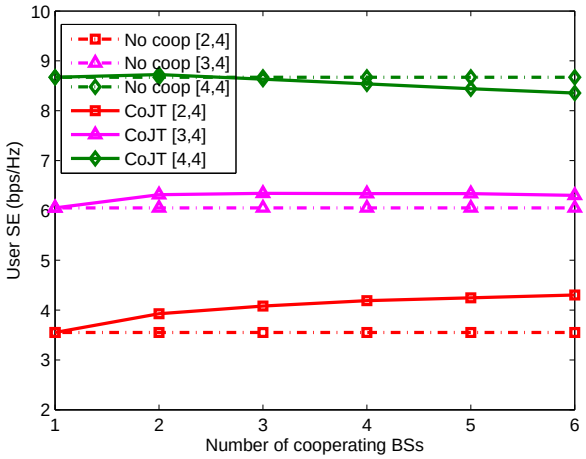

Figure 5.3: Cooperation gain with different dual-slope exponents $[\alpha_1, \alpha_2]$ when $\lambda_b = 4000/\text{km}^2$, $\lambda_u = 200/\text{km}^2$, $R_c = 70\text{m}$.

This trend is the same as the effect of critical distance aforementioned since increasing critical distance is equivalent with increasing UE density in the near-field. Regarding BS density, the cooperation gain can be divided into three regions: first decreases logarithmically, then decreases in a lower speed, and finally starts to in-

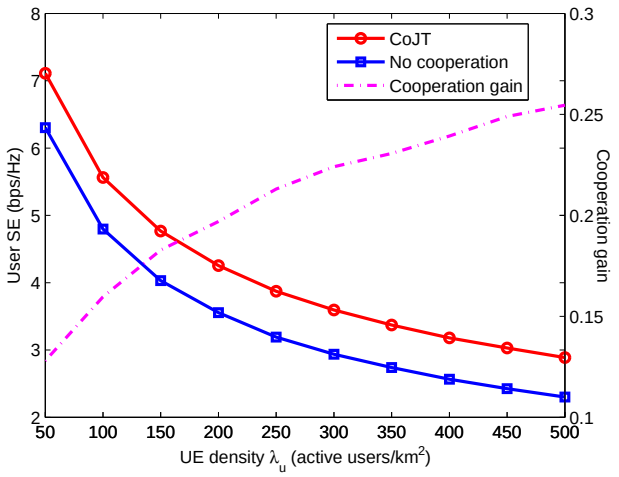

Figure 5.4: Cooperation gain with different UE densities when path loss exponents = [2,4], $\lambda_b = 4000/\text{km}^2$, $R_c = 70\text{m}$, $N = 5$.

crease after the BS density reaches a threshold. In region 1, the cooperation gain will decrease since the baseline will increase logarithmically with λ_b [28]. In region 2, the decreasing speed of the gain slows down because UEs start to enter the bounded region. Finally in region 3, the probability of $d_1 < R_b$ is quite high and $\mathcal{R}^o$ tends to be a constant. Therefore, the cooperation gain increases via further densification.

5.4 Summary

In this chapter, we evaluate two cooperation schemes in a UDN under a bounded dual-slope path loss model. Numerical results show that non-coherent JT even weakens the UE SE because the cooperative signal power cannot compensate for the additional interference. With the knowledge of CSI, coherent cooperative transmissions can provide SE gain depending on the environmental characteristics such as critical distance and path loss exponents. Meanwhile, the SE gain is an increasing function of UE density and a convex function of BS density (first decrease and then increase).

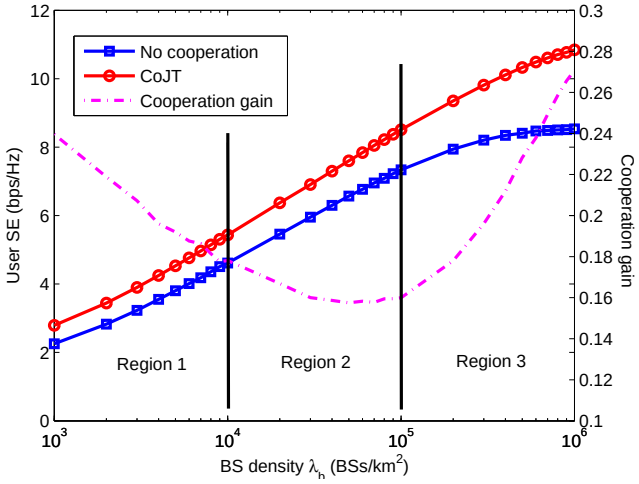

Figure 5.5: Cooperation gain with different BS densities when path loss exponents = [2,4], $\lambda_u = 200/\text{km}^2$, $R_c = 70\text{m}$, $N = 5$.

Chapter 6

Conclusion and Future Work

6.1 Concluding remarks

The upcoming data tsunami poses a tremendous challenge to the wireless industry and academia. In this thesis, we aim to provide analysis and guidelines from network densification perspective. To this end, we carry out a study on deployment and cooperative operations of a UDN.

We first investigate the resource trade-offs in network provisioning for both current macro-cellular network and future ultra-dense network. We compare the effectiveness of densification with the other two elements which can improve network capacity: spectrum expansion and multi-antenna systems. In current network deployment, densification outperforms the other two options. However, the gain of densification diminishes as BS density exceeds UE density which forms a UDN. In a UDN, acquiring more spectrum or installing multi-antennas are preferred than further densification. Furthermore, the importance of specifying UE demand is highlighted. Our results reveal that spectrum has a significant impact in achieving extreme high individual requirements while densification plays a more important role in accommodating massive UEs.

The diminishing gain appears in a UDN make us curious to know if there exists a terminal on the way of densification. Such uncertainty leads to the study on the asymptotic behavior of densification in the next part of the thesis. In order to capture the characteristics of a UDN, we apply a bounded dual-slope propagation and partial load model. Numerical results show that the coverage probability of the UE will neither drops to zero as some pessimistic predictions in references nor goes to infinity as we wish. Instead, it will converge to a finite value considering a certain UE density. Similarly, the ASE will converge as well under the same assumptions. Meanwhile, we find a rate-reliability trade-off during densification process which should draw attentions in network provisioning.

In the last part, we study cooperative transmissions in a UDN. By comparing schemes of non-coherent JT and coherent JT, we find that cooperation is not ben-

eficial without CSI in a UDN. With the CSI information, cooperation is favorable in UDN scenarios with longer critical distance and smaller path loss exponents. Moreover, employing cooperation is more effective in high UE density regions. On the contrary, high BS density is not helpful until it reaches the threshold and BSs fall into the bounded region.

6.2 Future works

In this thesis, most performance evaluations are based on single and omni-directional antenna assumptions. Current trend for system design is to install multi-antennas or form sharp beams in transmission. Incorporating these advance techniques will be preferable in UDNs as well. Meanwhile, the utilization of millimeter-wave (mmWave) has drawn great attention recently. The strong attenuation loss of mmWave can be made up by the short communication distances in a UDN environment. Therefore, mmWave and UDN could be a powerful combination. At last, ultra-reliable communication is becoming demanding in 5G and beyond. UDN may also make contribution to improve the system reliability in this field.

Bibliography

[1] "Strategies for mobile network capacity expansion," White Paper, RealWireless, Nov 2010.

[2] Ericsson, "Ericsson mobility report, on the pulse of the networked society," Tech. Rep., 2015.

[3] "5G systems," White Paper, Ericsson, January 2015.

[4] "The 1000x data challenge," White Paper, Qualcomm Incorporated, June 2013.

[5] "Looking ahead to 5G," White Paper, Nokia Solutions and Networks, Dec 2013.

[6] M. Dohler, R. W. Heath, A. Lozano, C. B. Papadias, and R. A. Valenzuela, "Is the phy layer dead?" *IEEE Communications Magazine*, vol. 49, no. 4, pp. 159–165, April 2011.

[7] F. Rusek, D. Persson, B. K. Lau, E. Larsson, T. Marzetta, O. Edfors, and F. Tufvesson, "Scaling up mimo: Opportunities and challenges with very large arrays," *Signal Processing Magazine, IEEE*, vol. 30, no. 1, pp. 40–60, Jan 2013.

[8] E. G. Larsson, O. Edfors, F. Tufvesson, and T. L. Marzetta, "Massive mimo for next generation wireless systems," *IEEE Communications Magazine*, vol. 52, no. 2, pp. 186–195, February 2014.

[9] N. Bhushan, J. Li, D. Malladi, R. Gilmore, D. Brenner, A. Damnjanovic, R. T. Sukhavasi, C. Patel, and S. Geirhofer, "Network densification: the dominant theme for wireless evolution into 5g," *IEEE Communications Magazine*, vol. 52, no. 2, February 2014.

[10] D. Lôpez-Pèrez, M. Ding, H. Claussen, and A. H. Jafari, "Towards 1 gbps/ue in cellular systems: Understanding ultra-dense small cell deployments," *IEEE Communications Surveys Tutorials*, vol. 17, no. 4, pp. 2078–2101, Fourthquarter 2015.

[11] Arraycomm. Cooper's law. [Online]. Available: http://www.arraycomm.com/technology/coopers-law/

[12] V. Chandrasekhar, J. G. Andrews, and A. Gatherer, "Femtocell networks: a survey," *IEEE Communications Magazine*, vol. 46, no. 9, pp. 59–67, September 2008.

[13] J. G. Andrews, "Seven ways that hetnets are a cellular paradigm shift," *IEEE Communications Magazine*, vol. 51, no. 3, pp. 136–144, March 2013.

[14] J. G. Andrews, H. Claussen, M. Dohler, S. Rangan, and M. C. Reed, "Femtocells: Past, present, and future," *IEEE Journal on Selected Areas in Communications*, vol. 30, no. 3, pp. 497–508, April 2012.

[15] R. Heath, S. Peters, Y. Wang, and J. Zhang, "A current perspective on distributed antenna systems for the downlink of cellular systems," *IEEE Communications Magazine*, vol. 51, no. 4, pp. 161–167, April 2013.

[16] C. S. Chen, V. M. Nguyen, and L. Thomas, "On small cell network deployment: A comparative study of random and grid topologies," in *2012 IEEE Vehicular Technology Conference (VTC Fall)*, Sept 2012, pp. 1–5.

[17] J. Huang, H. Zhang, W. Xu, and H. Zhang, "Grouping based inter-cell interference coordination in LTE-A dense small-cell networks," in *Microwave, Antenna, Propagation and EMC Technologies for Wireless Communications (MAPE), 2013 IEEE 5th International Symposium on*, Oct 2013, pp. 78–83.

[18] Y.-P. Zhang, S. Feng, P. Zhang, L. Xia, Y. chun Wu, and X. Ren, "Inter-cell interference management in LTE-A small-cell networks," in *Vehicular Technology Conference (VTC Spring), 2013 IEEE 77th*, June 2013, pp. 1–6.

[19] C. Li, J. Zhang, and K. Letaief, "Energy efficiency analysis of small cell networks," in *Communications (ICC), 2013 IEEE International Conference on*, June 2013, pp. 4404–4408.

[20] Y. S. Soh, T. Quek, M. Kountouris, and H. Shin, "Energy efficient heterogeneous cellular networks," *Selected Areas in Communications, IEEE Journal on*, vol. 31, no. 5, pp. 840–850, May 2013.

[21] R. Razavi and H. Claussen, "Urban small cell deployments: Impact on the network energy consumption," in *Wireless Communications and Networking Conference Workshops (WCNCW), 2012 IEEE*, April 2012, pp. 47–52.

[22] M. Coldrey, J. E. Berg, L. Manholm, C. Larsson, and J. Hansryd, "Non-line-of-sight small cell backhauling using microwave technology," *IEEE Communications Magazine*, vol. 51, no. 9, pp. 78–84, September 2013.

[23] D. C. Chen, T. Q. S. Quek, and M. Kountouris, "Backhauling in heterogeneous cellular networks: Modeling and tradeoffs," *IEEE Transactions on Wireless Communications*, vol. 14, no. 6, pp. 3194–3206, June 2015.

[24] J. Park, S.-L. Kim, and J. Zander., "Tractable resource management with uplink decoupled millimeter-wave overlay in ultra-dense cellular networks." [Online]. Available: http://arxiv.org/pdf/1507.08979.pdf

[25] J. Andrews, F. Baccelli, and R. Ganti, "A tractable approach to coverage and rate in cellular networks," *Communications, IEEE Transactions on*, vol. 59, no. 11, pp. 3122–3134, November 2011.

[26] X. Zhang and J. G. Andrews, "Downlink cellular network analysis with multi-slope path loss models," *IEEE Transactions on Communications*, vol. 63, no. 5, pp. 1881–1894, May 2015.

[27] J. Liu, M. Sheng, L. Liu, and J. Li, "Effect of densification on cellular network performance with bounded pathloss model," *IEEE Communications Letters*, vol. PP, no. 99, pp. 1–1, 2016.

[28] J. Park, S. L. Kim, and J. Zander, "Asymptotic behavior of ultra-dense cellular networks and its economic impact," in *2014 IEEE Global Communications Conference*, Dec 2014, pp. 4941–4946.

[29] Y. Yang and K. W. Sung, "Tradeoff between spectrum and densification for achieving target user throughput," in *Vehicular Technology Conference (VTC Spring), 2015 IEEE 81st*, May 2015, pp. 1–6.

[30] I. Hwang, B. Song, and S. Soliman, "A holistic view on hyper-dense heterogeneous and small cell networks," *Communications Magazine, IEEE*, vol. 51, no. 6, pp. 20–27, June 2013.

[31] H. S. Dhillon, R. K. Ganti, F. Baccelli, and J. G. Andrews, "Modeling and analysis of k-tier downlink heterogeneous cellular networks," *IEEE Journal on Selected Areas in Communications*, vol. 30, no. 3, pp. 550–560, April 2012.

[32] P. Marsch and G. Fettweis, "Static clustering for cooperative multi-point (comp) in mobile communications," in *2011 IEEE International Conference on Communications (ICC)*, June 2011, pp. 1–6.

[33] S. Catreux, P. F. Driessen, and L. J. Greenstein, "Simulation results for an interference-limited multiple-input multiple-output cellular system," *IEEE Communications Letters*, vol. 4, no. 11, pp. 334–336, Nov 2000.

[34] A. Ganz, C. M. Krishna, D. Tang, and Z. J. Haas, "On optimal design of multitier wireless cellular systems," *IEEE Communications Magazine*, vol. 35, no. 2, pp. 88–93, Feb 1997.

[35] A. D. Wyner, "Shannon-theoretic approach to a gaussian cellular multiple-access channel," *IEEE Transactions on Information Theory*, vol. 40, no. 6, pp. 1713–1727, Nov 1994.

[36] J. Xu, J. Zhang, and J. G. Andrews, "On the accuracy of the wyner model in cellular networks," *IEEE Transactions on Wireless Communications*, vol. 10, no. 9, pp. 3098–3109, September 2011.

[37] S. N. Chiu, D. Stoyan, W. S. Kendall, and J. Mecke, *Stochastic geometry and its applications*, 3rd ed. Wiley, 2013.

[38] E. N. Gilbert, "Random plane networks," *Journal of the Society for Industrial and Applied Mathematics*, vol. 9, no. 4, pp. 533–543, December 1961.

[39] F. Baccelli, M. Klein, M. Lebourges, and S. Zuyev, "Stochastic geometry and architecture of communication networks," *Telecommunication Systems*, vol. 7, no. 1, pp. 209–227, 1997.

[40] F. Baccelli and S. Zuyev, "Stochastic geometry models of mobile communication networks," in *Frontiers in queueing: models and applications in science and engineering*. CRC Press, 1996, pp. 227–243.

[41] S. M. Yu and S.-L. Kim, "Downlink capacity and base station density in cellular networks," in *Modeling Optimization in Mobile, Ad Hoc Wireless Networks (WiOpt), 2013 11th International Symposium on*, May 2013, pp. 119–124.

[42] C. Li, J. Zhang, and K. Letaief, "Throughput and energy efficiency analysis of small cell networks with multi-antenna base stations," *Wireless Communications, IEEE Transactions on*, vol. 13, no. 5, pp. 2505–2517, May 2014.

[43] D. Stoyan, W. Kendall, and J. Mecke, *Stochastic Geometry and Its Applications*. John Wiley and Sons, 1996.

[44] S. Lee and K. Huang, "Coverage and economy of cellular networks with many base stations," *Communications Letters, IEEE*, vol. 16, no. 7, pp. 1038–1040, July 2012.

[45] H. ElSawy, E. Hossain, and M. Haenggi, "Stochastic geometry for modeling, analysis, and design of multi-tier and cognitive cellular wireless networks: A survey," *IEEE Communications Surveys Tutorials*, vol. 15, no. 3, pp. 996–1019, Third 2013.

[46] G. Alfano, M. Garetto, and E. Leonardi, "New insights into the stochastic geometry analysis of dense csma networks," in *2011 Proceedings IEEE INFOCOM*, April 2011, pp. 2642–2650.

[47] METIS deliverable D1.1, "Scenarios, requirements and KPIs for 5G mobile and wireless system," April 2013.

[48] A. M. Hunter, J. G. Andrews, and S. Weber, "Transmission capacity of ad hoc networks with spatial diversity," *IEEE Transactions on Wireless Communications*, vol. 7, no. 12, pp. 5058–5071, December 2008.

[49] S. Sun, G. R. MacCartney, and T. S. Rappaport, "Millimeter-wave distance-dependent large-scale propagation measurements and path loss models for outdoor and indoor 5g systems," in *2016 10th European Conference on Antennas and Propagation (EuCAP)*, April 2016, pp. 1–5.

[50] V. Garcia, Y. Zhou, and J. Shi, "Coordinated multipoint transmission in dense cellular networks with user-centric adaptive clustering," *IEEE Transactions on Wireless Communications*, vol. 13, no. 8, pp. 4297–4308, Aug 2014.